J|A|C|S
ARTICLES

Published on Web 08/12/2009

Ammoniated Electrons Stabilized at the Surface of MgO

Mario Chiesa,* Elio Giamello, and Sabine Van Doorslaer

Dipartimento di Chimica IFM, Università di Torino and NIS, Nanostructured Interfaces and Surfaces Centre of Excellence, Via P. Giuria 7, I - 10125 Torino, Italy, and University of Antwerp, Department of Physics, Universiteitsplein 1, B-2610 Antwerp-Wilrijk, Belgium

Received April 21, 2009; E-mail: m.chiesa@unito.it

Abstract: The reaction of excess electrons at the surface of MgO with ammonia leads to surface ammoniated electrons analogous to those formed when alkali metals are dissolved in anhydrous ammonia. Surface excess electrons are found to be solvated by up to three ammonia molecules, and well-resolved CW and pulsed EPR spectra allow for a precise description of the unpaired electron spin density distribution over the solvent molecules. The large majority of the electron spin density resides in the first-shell nitrogen fragments. HYSCORE spectra allow obtaining for the first time the full hyperfine interaction of the solvated electron with the ammonia protons, which is consistent with a small and negative spin density in the ^{1}H 1s orbital. Furthermore, the hyperfine and nuclear quadrupole tenors of the second-shell nitrogens could be unravelled.

1. Introduction

The brilliant blue color of metal ammonia solutions attracted the attention of both chemists and physicists ever since the discovery that alkali metals dissolve in pure liquid ammonia to yield solvated cations and unique "solvated electrons".[1,2] Solvated electrons are remarkable chemical entities, which are still at the forefront of research activity due to their peculiar properties and yet to come possible applications.[3] Substantial experimental and theoretical efforts have been produced to elucidate their microscopic structure and dynamics, which succeeded in producing a fairly detailed picture of solvated electrons in homogeneous media,[4] even though complete understanding of their structure and properties remains somewhat evasive.[5] This is particularly true when excess electron localization takes place at surfaces and interfaces.

Just as they can be introduced into protic solvents, excess electrons can be stabilized on two-dimensional surfaces.[6−8] The localization of excess electrons at surfaces and interfaces is not only a stimulating academic research area but also an important topic of technological significance due to the potential role of these entities in affecting properties such as charge injection and transport at interfaces. This makes surface-solvated electrons prominent actors in interfacial photo processes, particularly in photoelectrochemistry and photocatalysis,[9−11] and many studies focused on the investigation of the electron transfer and solvation dynamics at various molecule−metal interfaces[12−14] by means of surface-science techniques, aimed to address fundamental questions concerning electron solvation and its dynamics in two-dimensional environments.[6,15,16]

Electron solvation has also been observed in the case of ionic insulators, such as zeolites[17] or alkaline-earth oxides.[8] These materials can be regarded as polar solid solvents where the elementary mechanisms, which are at the basis of the generation of solvated electrons in condensed media, lead to the generation of "electron-rich" surfaces.

The case of alkaline-earth-oxide surfaces is particularly interesting as they can act as two-dimensional polar matrixes, and appealing similarities can be found between the chemistry of the surface and solution chemistry. An interesting example is the case of the interaction of alkali-metal atoms with the surface of MgO, where, similarly to classical solvation, the resulting species may be regarded as an "expanded atom" whereby specific surface sites act as solvating agents.[18]

MgO is a prototypical example of an ionic and insulating oxide and has been widely employed for fundamental investigations.[19] This oxide has a simple NaCl structure and is characterized by morphological defective features such as steps, corners

(1) Edwards, P. P. *J. Supercond.* **2000**, *13*, 933.
(2) Edwards, P. P. *Adv. Inorg. Chem. Radiochem.* **1982**, *25*, 135–185.
(3) Edwards, P. P.; Rao, C. N. R.; Kumar, N.; Alexandrov, A. S. *ChemPhysChem* **2006**, *7*, 2015.
(4) Lee, I. R.; Lee, W.; Zewail, A. H. *ChemPhysChem* **2008**, *9*, 83.
(5) Shkrob, I. A. *J. Phys. Chem. A* **2006**, *110*, 3967.
(6) Zhao, J.; Li, B.; Onda, K.; Feng, M.; Petek, H. *Chem. Rev.* **2006**, *106*, 4402.
(7) Miller, A. D.; Bezel, I.; Gaffney, K. J.; Garrett-Roe, S.; Liu, S. H.; Szymanski, P.; Harris, C. B. *Science* **2002**, *297*, 1163.
(8) Chiesa, M.; Paganini, M. C.; Giamello, E.; Murphy, D. M.; Di Valentin, C.; Pacchioni, G. *Acc. Chem. Res.* **2006**, *39*, 861.
(9) Nitzan, A. *Chemical Dynamics in Condensed Phases*; Oxford University Press: Oxford, 2006.
(10) Onda, K.; Li, B.; Zhao, J.; Jordan, K. D.; Yang, J. L; Petek, H. *Science* **2005**, *308*, 1154.
(11) Gundlach, L.; Ernstorfer, R.; Willig, F. *Prog. Surf. Sci.* **2007**, *82*, 161.
(12) Szymanski, P.; Garrett-Roe, S.; Harris, C. B. *Prog. Surf. Sci.* **2005**, *78*, 1.
(13) Ge, N.-H.; Wong, C. M.; Harris, C. B. *Acc. Chem. Res.* **2000**, *33*, 111.
(14) Stähler, J.; Meyer, M.; Kusmierek, D. O.; Bovensiepen, U.; Wolf, M. *J. Am. Chem. Soc.* **2008**, *130*, 8797.
(15) Harris, C. B. *J. Phys. Chem. B* **2005**, *109*, 20370.
(16) Stähler, J.; Bovensiepen, U.; Meyer, M.; Wolf, M. *Chem. Soc. Rev.* **2008**, *37*, 2180.
(17) Edwards, P. P.; Anderson, P. A.; Thomas, J. M. *Acc. Chem. Res.* **1996**, *29*, 23.
(18) Chiesa, M.; Giamello, E.; Di Valentin, C.; Pacchioni, G.; Sojka, Z.; Van Doorslaer, S. *J. Am. Chem. Soc.* **2005**, *127*, 16935.

10.1021/ja903179b CCC: $40.75

or reverse corners, which are known to be dominant irregularities at the surface of oxide polycrystals as well as thin oxide films.

We recently reported a new class of surface defects generated by the interaction of atomic hydrogen with the clean surface of MgO, which can be described in terms of an excess electron−proton pair stabilized at low coordinated surface sites. Exposure of MgO[20−23] or CaO[24] surfaces to H atoms or to H_2 under UV light results in the spontaneous ionization of $H^{\bullet}$ at temperatures as low as 77 K with the subsequent formation of excess electrons and extra protons on the surface, as schematically represented in eq 1.

$$H^{\bullet} + \text{–Mg–O–} \xrightarrow{e^-\ \ H^+} \text{–Mg–O–} \qquad (1)$$

These centers are named $(H^+)(e^-)$[20] and result from the ionization of the H atom with subsequent stabilization of the electron on low-coordinated cation sites (mainly corners and steps), and of the proton on surface oxide anions. Reaction 1 leads to surface excess electron color centers thermally stable up to 373 K, fully characterized by EPR-, IR-, and UV measurements, and theoretical calculations. These functionalized electron-rich surfaces display a number of fascinating optical and magnetic properties[25] and feature a remarkable chemical reactivity acting as powerful reducing agents (N_2^-, CO_2^-).[26−28]

Taking a lead from an observation of Symmons and Wardman,[29] we report a detailed continuous-wave (CW) and pulse EPR study on the reactivity of surface excess electron centers on MgO with ammonia. When ammonia is contacted with these centers, dramatic changes in both the EPR and optical absorption are observed, which are characteristic of so-called "ammoniated electrons".[30] Our aim is to provide a precise description of the electron spin-density distribution in the surface ammonia-solvated electrons. To do so, we will exploit the MgO surface as a bidimensional ionic matrix to isolate ammoniated electrons, which will allow overcominge the main problems of solvated electrons in liquid media, namely the motional averaging, which lead to unresolved EPR spectra. We will show that the so-formed surface-isolated solvated electrons capture the essential features of solvated electrons in ammonia and provide a model system for electron solvation in its embryonic stages. Despite a huge body of experimental and theoretical works, a detailed microscopic picture of solvated electrons is still lacking. The widely accepted model for these chemical entities is that excess electrons reside within solvent cavities. Recent computational work on gas-phase ammoniated electrons[5] and Li−ammonia solutions[31] suggest, however, that the electrons do not reside within the voids but rather at the void−solvent interface. Our new experimental data concur with this last model.

Current models of solvated electrons are largely based on data coming from magnetic resonance techniques. In particular, the description of the spin-density distribution over the solvent molecules for ammoniated electrons is mainly based on detailed NMR studies of solvated electrons in methylamine using the ^{1}H and ^{14}N Knight shift data.[32] The Knight shift represents the summation of all interactions averaged over all the nuclei encompassed within the unpaired electron wave function and provides only the Fermi contact interaction. The NMR analysis thus reveals only the Fermi contact term (a_{iso}), failing to detect the anisotropic part of the hyperfine tensor. Moreover, specific model distributions need to be applied in order to establish the spread of the unpaired electron density over the different coordinating shells. In this way, ^{14}N isotropic hyperfine couplings of the order of 34 MHz for the primary shell and 9 MHz for the secondary shell of solvents have been proposed.[33] Values in line with the above-reported estimates for the first ^{14}N shell were reported in the past by Wardman and Symmons.[29] However, contrary to the first-shell ^{14}N hyperfine coupling, the ^{1}H proton hyperfine coupling and the second-shell ^{14}N coupling have never been directly detected via EPR, and current models rely on estimates deduced from NMR experiments. One of the major outcomes of the present study is to provide for the first time the precise details of the unpaired electron distribution for surface ammoniated electrons obtaining the fully resolved ^{1}H hyperfine coupling tensor for the first ammonia shell and the ^{14}N hyperfine and quadrupolar tensors for the secondary shell. Analysis of these data strongly supports a model where the excess electron is "spread" over the ammonia nitrogens rather than confined within solvent cavities, in agreement with recent calculations.[5,31]

2. Experimental Section

High surface area MgO (200 $m^2\ g^{-1}$) was obtained by slow thermal decomposition under dynamic vacuum of the corresponding hydroxide (*Aldrich*). The oxide was then activated at 1173 K for 1 h. The hydrogen atoms were produced in a 2.45 GHz microwave discharge under static conditions. Typical hydrogen pressure was 0.3 mbar.

2.1. CW-EPR. Spectra were recorded on a Bruker EMX spectrometer operating at X-band frequencies and equipped with a cylindrical cavity operating at a 100 kHz field modulation. The spectra have been recorded at 1 mW microwave power. The sample was cooled by a gas-flow cryostat operated from $T = 4.0$ to 300 K. DPPH ($g = 2.0036$) and a solid solution of Mn^{2+} in MgO ($g = 2.0064$) have been used as standards for g-value calibration.

2.2. Pulse EPR. Experiments were performed with an ESP380E Bruker spectrometer (microwave (mw) frequency 9.76 GHz) equipped with a liquid-helium cryostat from Oxford Inc. All experiments were done at 12 K and a repetition rate of 100 Hz. The magnetic field was measured with a Bruker ER035 M NMR Gaussmeter.

2.3. Electron Spin−Echo (ESE) Detected EPR. The experiments were carried out with the pulse sequence: $\pi/2 - \tau - \pi - \tau$-echo, with mw pulse lengths $t_{\pi/2} = 16$ ns and $t_\pi = 32$ ns and a

(19) Spoto, G.; Gribov, E. N.; Ricchiardi, G.; Damin, A.; Scarano, D.; Bordiga, S.; Lamberti, C.; Zecchina, A. *Prog. Surf. Sci.* **2004**, *76*, 71.
(20) Ricci, D.; Di Valentin, C.; Pacchioni, G.; Sushko, P. V.; Shluger, A. L.; Giamello, E. *J. Am. Chem. Soc.* **2003**, *125*, 738.
(21) Chiesa, M.; Paganini, M. C.; Giamello, E.; Di Valentin, C.; Pacchioni, G. *Angew. Chem., Int. Ed.* **2003**, *42*, 1759–1761.
(22) Chiesa, M.; Paganini, M. C.; Spoto, G.; Giamello, E.; Di Valentin, C.; Del Vitto, A.; Pacchioni, G. *J. Phys. Chem. B* **2005**, *109*, 7314–7322.
(23) Smith, D. R.; Tench, A. J. *Chem. Commun.* **1968**, 1113.
(24) Chiesa, M.; Paganini, M. C.; Giamello, E.; Di Valentin, C.; Pacchioni, G. *ChemPhysChem* **2006**, *7*, 728–734.
(25) Moreira, I. D. P. R.; Wojdel, J. C.; Illas, F.; Chiesa, M.; Giamello, E. *Chem. Phys. Lett.* **2008**, *462*, 78.
(26) Chiesa, M.; Giamello, E.; Murphy, D. M.; Pacchioni, G.; Paganini, M. C.; Soave, R.; Sojka, Z. *J. Phys. Chem. B* **2001**, *105*, 497.
(27) Chiesa, M.; Giamello, E. *Chem.−Eur. J.* **2007**, *13*, 1261.
(28) Preda, G.; Pacchioni, G.; Chiesa, M.; Giamello, E. *J. Phys. Chem. C* **2008**, *112*, 19568.
(29) Smith, D. R.; Symmons, M. C. R.; Wardman, P. *J. Phys. Chem.* **1979**, *83*, 1762.
(30) Kraus, C. A. *J. Am. Chem. Soc.* **1908**, *30*, 1323.
(31) Chandra, A.; Marx, D. *Angew. Chem., Int. Ed.* **2007**, *46*, 3676.
(32) Holton, D. M.; Edwards, P. P.; McFarlane, W.; Wood, B. *J. Am. Chem. Soc.* **1983**, *105*, 2104.
(33) Symons, M. C. R. *Chem. Soc. Rev.* **1976**, 337.

τ value of 200 ns. The EPR computer simulations were performed using the EPRSIM32 program.[34]

2.4. Three-Pulse ESEEM (Electron Spin−Echo Envelope Modulation). Experiments were carried out using the pulse sequence $\pi/2 - \tau - \pi/2 - T - \pi/2 - \tau$-echo with mw pulses of length $t_{\pi/2} = 16$ ns, a starting time $T_0 = 96$ ns and a time increment $\Delta T = 16$ ns (512 intervals). In order to remove blind spots time τ was increased in steps of 8 ns from 96 to 216 ns.

2.5. Matched Three-Pulse ESEEM.[35] Experiments have been carried out using the sequence $\pi/2 - \tau - (HTA) - T - (HTA) - \tau$-echo, where the matching pulse field strength ν_1 was taken to be 15.625 MHz. The length of the high turning angle (HTA) pulse was optimized by incrementing the pulse length of the second and third pulses in steps of 8 ns starting from 16 ns. The optimal value of the HTA pulse was found to be 96 ns

2.6. Hyperfine Sublevel Correlation (HYSCORE).[36] Experiments were carried out with the pulse sequence $\pi/2 - \tau - \pi/2 - t_1 - \pi - t_2 - \pi/2 - \tau$-echo with mw pulse length $t_{\pi/2} = 16$ ns and $t_\pi = 16$ ns. The time intervals t_1 and t_2 were varied in steps of 16 ns starting from 96 to 3288 ns. Two different τ values were chosen ($\tau = 96$ and 176 ns). An eight-step phase cycle was used to eliminate unwanted echoes.

UV−vis−NIR (Varian Cary-5) spectra were recorded *in situ* on the same sample employed for the EPR analysis using a quartz cell equipped with both a cell for optical measurements and an EPR tube.

2.7. Matched HYSCORE experiments.[37] were carried out with the sequence $\pi/2 - \tau - (HTA) - t_1 - \pi - t_2 - (HTA) - \tau$-echo. Settings of the HTA matching pulses were the same as for the matched three pulse ESEEM experiments. The time traces of the HYSCORE spectra were baseline corrected with a third-order polynomial, apodized with a Hamming window and zero filled. After two-dimensional Fourier transformation, the absolute value spectra were calculated. The spectra were added for the different τ values in order to eliminate blind-spot effects. The HYSCORE spectra were simulated using a program developed at the ETH Zurich.[38]

3. Results and Discussion

3.1. The NH_3 Interaction with MgO. Atomic hydrogen undergoes spontaneous ionization over surface morphological features of MgO leading to surface excess electron−proton pairs stabilized at low-coordinated $Mg^{2+}-O^{2-}$ ions. The CW-EPR spectrum of $(H^+)(e^-)$ centers (Figure 1a) is dominated by an axial feature with $g_\perp = 1.999$ and $g_\parallel = 2.001$ and is primarily characterized by a resolved doublet hyperfine splitting of about 6 MHz. This splitting arises from the magnetic interaction between the unpaired electron and the H nucleus of a neighboring OH^- group. Also a six-line hyperfine pattern with separation of about 28 MHz due to the superhyperfine interaction of the unpaired electron with ^{25}Mg nuclei ($I = 5/2$, abundance = 10%) is detected in the spectrum. All these features have been thoroughly discussed elswhere.[8] $(H^+)(e^-)$ centers are also characterized by an optical spectrum distinguished by an absorption pattern (Figure 1d), dominated by two absorption bands with maximum at 1250 and 730 nm. Annealing experiments show that these absorption features are correlated to the CW-EPR spectrum shown in Figure 1a.

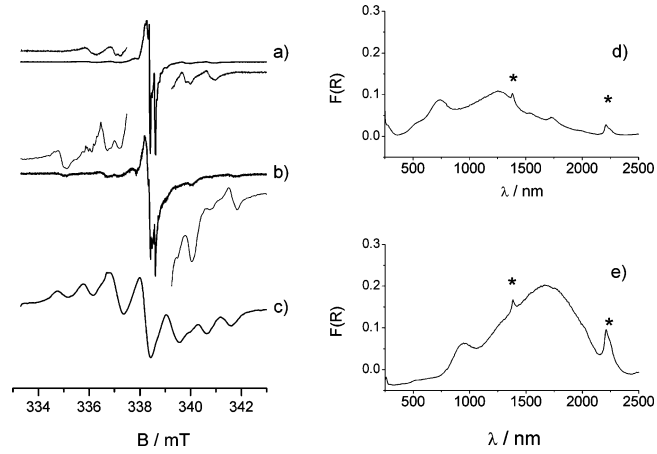

Figure 1. (a) CW-EPR spectrum of $(H^+)(e^-)$ centers on MgO; (b) CW-EPR spectrum observed after the adsorption of 0.1 mbar of NH_3; (c) CW-EPR spectrum recorded after the adsorption of 0.8 mbar of NH_3;(d) UV−vis−NIR absorption of $(H^+)(e^-)$ centers on MgO; (e) UV−vis−NIR absorption after adsorption of 1 mbar of $^{14}NH_3$ on $(H^+)(e^-)$ centers. All CW-EPR and UV−vis−NIR absorption spectra are taken at room temperature. The asterisks in the UV−vis−NIR spectra indicate instrumental artifacts.

When ammonia (0.1 mbar) is contacted with the electron-rich MgO sample, a modification in the CW-EPR spectrum is observed (Figure 1b), and overamplification of the spectral wings reveals a five-line hyperfine pattern with separation of about 45 MHz. Increasing the dose of adsorbed ammonia (0.8 mbar) leads to a new spectrum characterized by a well-resolved seven-line hyperfine pattern as shown in Figure 1c. Further increase in the ammonia dose leads to a broad unresolved line and eventually to disappearance of the spectrum. Together with the appearance of the new EPR spectrum upon ammonia adsorption, a color change in the sample is observed, which results from a marked red shift in the absorption spectrum of the electron-rich MgO sample. The UV−vis−NIR spectrum corresponding to the 7-line CW-EPR spectrum is shown in Figure 1e and is dominated by a broad and pronounced band centered at about 1650 nm (0.74 eV), which is characteristic of solvated electrons in ammonia.[2]

The new CW-EPR spectrum obtained upon ammonia adsorption is characterized by seven equally spaced lines with average separation of about 30 MHz and relative line amplitudes 1:3:6:7:6:3:1 and is stable upon pumping the system in vacuum.

This result can be interpreted in terms of the interaction of the unpaired electron with three equivalent ^{14}N nuclei ($I = 1$). Computer simulation of the spectrum (Figure 2), however, revealed that the spectral pattern is best reproduced if together with the 7-line spectrum, a contribution due to a 5-line spectrum (2 equivalent N nuclei) is taken into account. This last species, due to the interaction of the unpaired electron with two equivalent nitrogen nuclei, was clearly observable in the spectrum reported in Figure 1b, in the presence of low ammonia coverages. The presence of this species is confirmed by isotopic substitution with $^{15}NH_3$ (^{15}N, $I = 1/2$). The spectrum observed upon interaction of $(H^+)(e^-)$ centers with $^{15}NH_3$, shown in Figure 2c, is characterized by four lines with intensity ratio 1:3:3:1 and a central line, which arises from the presence of a triplet of lines with intensity ratio 1:2:1 as expected for two equivalent nuclei with $I = 1/2$. The simulation of the $^{15}NH_3$ spectrum was obtained by scaling the hyperfine coupling constants deduced for the $^{14}NH_3$ spectrum by the ratio between ^{15}N and ^{14}N magnetic moments. From the computer simulations, the con-

(34) Spalek, T.; Pietrzyk, P.; Sojka, Z. *J. Chem. Inf. Model.* **2005**, *45*, 18.
(35) Schweiger, A.; Jeschke, G. *Principles of Pulse Electron Paramagnetic Resonance*; Oxford University Press: Oxford, U.K., 2001.
(36) Höfer, P.; Grupp, A.; Nebenfür, H.; Mehring, M. *Chem. Phys. Lett.* **1986**, *132*, 279.
(37) Jeschke, G.; Rakhmatulin, R.; Schweiger, A. *J. Magn. Reson.* **1998**, *131*, 261.
(38) Madi, Z. L.; Van Doorslaer, S.; Schweiger, A. *J. Magn. Reson.* **2002**, *154*, 187.

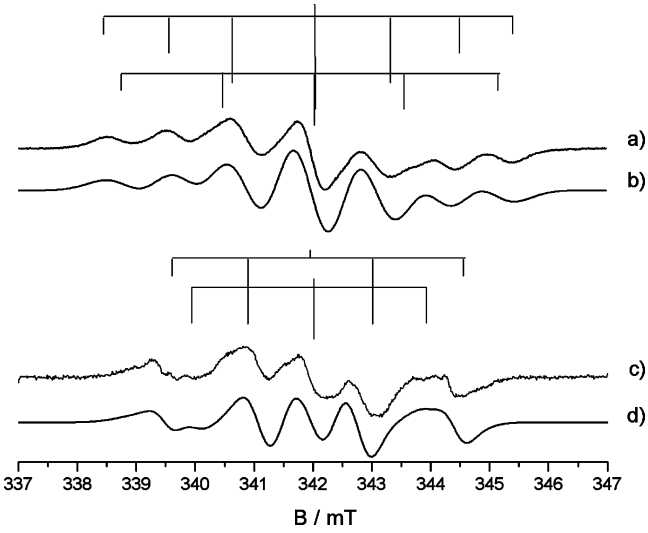

Figure 2. Experimental (a) and simulated (b) CW-EPR spectra of surface ammoniated electrons obtained by adsorption of 0.8 mbar of $^{14}NH_3$. (c,d) Experimental (c) and simulated (d) CW EPR spectra obtained by adsorption of 0.8 mbar of $^{15}NH_3$. The spectra were recorded at 77 K.

Table 1. Spin Hamiltonian Parameters for the Different Surface Ammoniated Electrons Extracted from the Computer Simulation Reported in Figure 2

species	$g_{\|}$	$g_{\perp}$	$\|A_{\|}\|$/MHz	$\|A_{\perp}\|$/MHz
$(NH_3)_3^-$	2.000 ± 0.0003	1.999 ± 0.0003	30.8 ± 2.0	28.4 ± 2.0
$(NH_3)_2^-$	2.000 ± 0.0003	1.999 ± 0.0003	44.8 ± 2.0	40.6 ± 2.0

tribution of the 'two equivalent nitrogen' species was estimated to be only about 5% of the total contribution. However, this contribution is strongly dependent on the ammonia pressure and was found to slightly change from one experiment to the other. Moreover, in the low pressure regime the 'two equivalent nitrogen' contribution was found to be more pronounced at room temperature with respect to low temperature. We argue that the "three equivalent nitrogen" species represents the more stable situation and we will focus on this species in the following. The spin Hamiltonian parameters of the two species were obtained from computer simulation of the spectra (in Figure 2) and are reported in Table 1. The small degree in anisotropy in both **g** and **A** tensors was established by means of computer simulation and corresponds to the maximum anisotropy that could be imposed, given the line width of the spectrum (0.5 mT). These values thus represent an upper limit. On the basis of these values, isotropic hyperfine (a_{iso}) values of 42.0 and 29.2 MHz are extracted for the two-ammonia and three-ammonia solvated electron centers, respectively, while $T = 1.4$ MHz and $T = 0.8$ MHz are the corresponding dipolar contributions. The small T values indicate that, even though a small dipolar character is acquired by the electron−ammonia complex, the SOMO is predominantly *s* in character.

Similar results were observed when ammonia was previously adsorbed on the surface of MgO and subsequently exposed to UV irradiation, in good agreement with what is reported in the literature.[29]

From the above-reported results it clearly emerges that the excess electron forms a complex with two or three ammonia groups stabilized at the surface depending on the ammonia coverage. We believe that this surface-isolated electron−ammonia complex can be considered as the archetypal of the ammoniated electron and thus represents *the core* of the excess electrons in

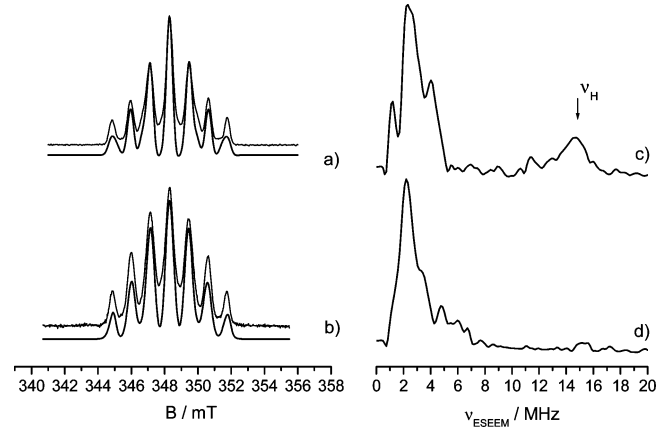

Figure 3. (a) ESE-detected EPR spectrum of surface ammoniated electrons observed upon adsorption of NH_3 on $(D^+)(e^-)$ centers; (b) ESE-detected EPR spectrum observed upon adsorption of ND_3 on $(H^+)(e^-)$ centers. (c) ^1H matched three-pulse ESEEM spectrum in the frequency domain for spectrum (a); (d) ^1H matched three-pulse ESEEM spectrum in the frequency domain for spectrum (b). The ESEEM spectra were taken at 348.2 mT, observer position corresponding to the central peak of the ESE spectra. The proton Larmor frequency (ν_H) is indicated in the frequency domain spectra.

liquid ammonia. The details of this model will be discussed in the following.

3.2. The Proton Hyperfine Coupling. As anticipated in the Introduction no direct measure of proton hyperfine coupling exists for ammoniated electrons. Data are however available from NMR Knight shifts, which unambiguously point to a small and negative spin density at the ammonia protons. In agreement with these studies no hyperfine proton coupling could be detected in the CW-EPR spectra and experiments performed with ND_3 did not lead to appreciable variations in the line width, indicating that the proton hyperfine interaction is indeed too small to be detected by this technique.

Pulsed EPR experiments were thus performed in order to characterize the proton hyperfine coupling, which, to the best of our knowledge, has never been measured directly for the ammoniated electron. Since the excess electron centers are generated using hydrogen and are characterized by a weak proton hyperfine coupling, isotopic substitution is necessary in order to discriminate between the hyperfine coupling with the original OH group and the NH_3 protons. Experiments were thus performed generating the excess electron centers using D ($I = 1$ $g_n = 0.8574376$) and subsequently contacting it with NH_3 and, *vice versa*, generating the centers using H and contacting it with ND_3. In particular, in order not to miss important features relative to the proton coupling and to enhance the intensity of the ESEEM spectrum, ^1H-matched three-pulse ESEEM spectra were recorded, which are reported in Figure 3 along with the ESE-detected EPR spectra for the two different isotopic compositions. The ESEEM spectra reported in Figure 3 were recorded at an observer position of 348.2 mT corresponding to the central line of the EPR spectrum. The same results were observed for other magnetic field settings, at which only the three nitrogen species contribute to the spectrum, ensuring that the ESEEM results refer to electrons solvated by three ammonia molecules. Spectra a and b of Figure 3 show the ESE-detected EPR spectra for the D/NH_3 and H/ND_3 system, respectively. The two spectra are substantially similar. On the contrary, the three-pulse ESEEM spectra show clear differences in the frequency domain spectrum, in particular the presence of a broad signal centered at the proton Larmor frequency in the case of

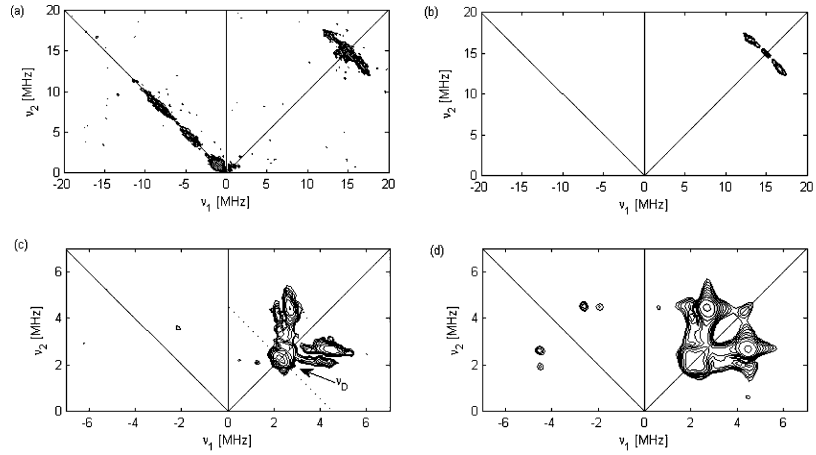

Figure 4. (a) Matched proton HYSCORE spectrum of ammoniated electrons observed upon adsorption of NH_3 on $(D^+)(e^-)$ centers; (b) computer simulation of spectrum (a); (c) standard HYSCORE spectrum of ammoniated electrons observed upon adsorption of NH_3 on $(D^+)(e^-)$ centers; (d) computer simulation of spectrum (c).

Table 2. Proton and Nitrogen Hyperfine and Nitrogen Nuclear Quadrupolar Constants Used in the Computer Simulation of the HYSCORE Spectra Reported in Figure 4

$\lvert^1H A_\parallel\rvert$/MHz	$\lvert^1H A_\perp\rvert$/MHz	$\lvert^{14}N A_\parallel\rvert$/MHz	$\lvert^{14}N A_\perp\rvert$/MHz	$\lvert e^2qQ/h\rvert$/MHz	η
5.55 ± 0.05	4.05 ± 0.05	1.7 ± 0.05	1.1 ± 0.05	3.2 ± 0.1	0.25 ± 0.05

Chart 1. Schematic Illustration of the Second Ammonia Shell[a]

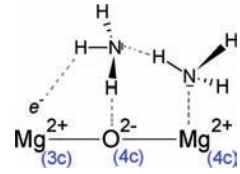

[a] For the sake of clarity only a single MgO edge is shown.

the D/NH_3 system, which is absent in the H/ND_3 sample. This broad peak is associated to a weak proton hyperfine interaction, which must arise from the surface NH_3 groups forming the trapping cage.

In order to better resolve the ^1H coupling and to extract the hyperfine coupling tensor, matched proton HYSCORE experiments were carried out for the $(D^+)(e^-)/NH_3$ system. The spectrum is shown in Figure 4a and consists of a pronounced ridge in the (+,+) quadrant with maximum extension of about 5.5 MHz, centered at the ^1H Larmor frequency. Considering that the maximum extension of the ridge corresponds to $|a_{iso} + 2T|$ and that the maximum displacement of the proton HYSCORE ridge from the diagonal peak (ν_H, ν_H) depends directly on the magnitude of T,[39] the values of a_{iso} and T can be determined. Assuming the sign of T as positive (g_n for H is positive) and a negative a_{iso} (as derived from NMR data), the values of $a_{iso} = -0.85$ MHz and $T = 3.15$ MHz were obtained by means of computer simulation of the spectrum (Figure 4b). These values are in fairly good agreement with models derived from the NMR Knight shift data[40] and in line with recently calculated values reported by Shkrob for gas-phase trimeric ammonia cluster anions.[5]

HYSCORE experiments were then performed on the $(H^+)(e^-)/ND_3$ system. In agreement with three-pulse ESEEM experiments, no proton ridge was observed in matched HYSCORE experiments (not shown), while a complex spectral pattern is recorded in the (+,+) quadrant of the standard HYSCORE spectrum (Figure 4c). The spectrum contains a ridge centered at the ^2H Larmor frequency (indicated in Figure 4c), which can be nicely simulated using the parameters deduced from the simulation of the ^1H ridge (Table 2) and accounting for the different nuclear spin and nuclear magnetic moment of D. No sign of D quadrupolar splitting is observed in the HYSCORE spectrum, and computer simulation of the spectrum indicates an $|e^2qQ/h|$ value smaller than 0.3 MHz. This is in agreement with the small value of the quadrupole interaction of deuterium in polycrystalline ND_3, which has been reported to be 156 ± 7 kHz.[41] Moreover, two cross-peaks centered at (2.7, 4.3) MHz and (4.3, 2.7) MHz are present, which arise from the interaction of the unpaired electron with distant (second shell) nitrogens. Simulation of these features could be obtained by considering a set of weakly coupled nitrogens, characterized by the hyperfine tensor elements reported in Table 2. Assuming all the signs to be positive, an a_{iso} value of 1.3 MHz and a dipolar coupling constant T of 0.2 MHz can be obtained. The alternative with all negative signs leads to a negative a_{iso}, which contradicts the NMR indications.[32,40] The ridges in the experimental spectrum are due to double-quantum transitions of the nitrogen and could be reproduced by imposing a fairly large and anisotropic nuclear quadrupolar interaction with quadrupole coupling constant $|e^2qQ/h| = 3.2$ MHz and an asymmetry parameter η of 0.25. This quadrupole coupling constant value is in line with that expected for ammonia, for which a value of 4.09 MHz was measured in the gas phase.[42] The reduction with respect to the gas-phase value can be rationalized considering the hydrogen bond interaction with the first ammonia shell (see Chart 1)

3.3. The Nature of Ammoniated Electrons on MgO. On the basis of the above-reported evidence a tentative model can be proposed for the surface ammoniated electron on MgO. At low ammonia coverage two equivalent nitrogen nuclei are found to be interacting with the unpaired electron. However, by increasing the number of adsorbed ammonia molecules, the septet spectrum due to three equivalent N nuclei becomes dominant. The magnetic equivalence for the three nitrogen atoms clearly

(39) Pöppl, A.; Kevan, L. *J. Phys. Chem.* **1996**, *100*, 3387.
(40) Niibe, M.; Nakamura, Y. *J. Phys. Chem.* **1984**, *88*, 5608.
(41) Rabideau, S. W.; Waldstein, P. *J. Chem. Phys.* **1966**, *45*, 4600.
(42) Kukolich, S. G.; Wopsy, S. C. *J. Chem. Phys.* **1970**, *52*, 5477.

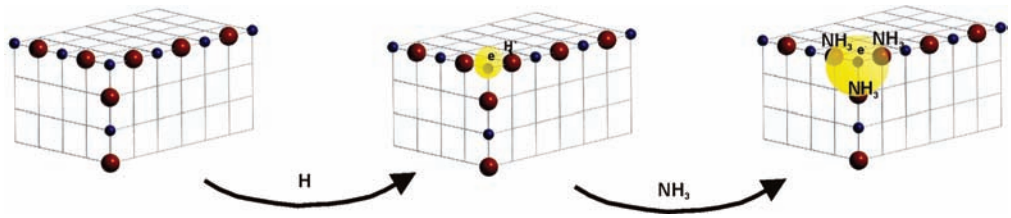

Figure 5. Schematic model showing the generation of $(H^+)(e^-)$ centers and the formation of surface ammoniated electrons at corner sites of MgO. The yellow volume represents the confinement space of the unpaired electron. Only the first ammonia shell is shown.

puts serious constraints to the possible hosting sites, restricting candidates to corner sites, where a C_{3v} axis of symmetry is present.

In the following we will focus on the trimeric ammonia−electron centers. Further structural details on the structure of surface ammoniated electrons can be obtained by the proton hyperfine tensor derived from HYSCORE spectra. Assuming the anisotropic part of the hyperfine interaction can be described as a purely point dipolar interaction, the distance between the proton and the center of mass of the unpaired electron can be estimated to be about 0.29 nm from eq 2.

$$T = \frac{\mu_0}{4\pi} g_e g_n \beta_e \beta_n \frac{1}{r^3} \tag{2}$$

Even though the use of this point dipolar approximation can lead to significant errors in the present case where a consistent spin density is present on the nitrogen nuclei, the obtained value for the proton−electron distance is approximately in the order of the distance (0.19−0.24 nm) calculated by Shkrob[5] for trimeric gas-phase anion clusters. Considering, then, the MgO lattice parameter (0.41 nm), simple geometrical arguments indicate that the excess electron is trapped at a three-coordinated (corner) Mg^{2+} cation and surrounded by three ammonia molecules adsorbed to the nearest O^{2-} or OH^- groups. It is in fact known that NH_3 molecularly adsorbs on surface oxide and hydroxyl anions as well as onto surface Mg^{2+} cations.[43,44] Our experiments do not allow discrimination between these two situations; however, they clearly demonstrate that the $(NH_3)_3^-$ fragment is stabilized by the strong electrostatic potential exerted by three-coordinated Mg^{2+} ions as already shown in the case of $(H^+)(e^-)$ centers.[21]

A pictorial model for the surface ammoniated electron as derived from the above considerations is shown in Figure 5, where the electron density is confined within a cage formed by three equivalent surface-stabilized ammonia molecules located at the edges of the MgO nanocubes. It is noteworthy that, considering the MgO lattice parameter, the cavity radius formed by the NH_3 fragments is compatible with the 0.3 nm radius for the cavity model proposed by Jortner[45] for solvated electrons in anhydrous ammonia.

The cavity model for the ammoniated electrons was first suggested by Ogg[46] and later developed by Jortner,[45] and is based on an idealized particle-in-a-box approach where the excess electron dwells in a cavity generated by the Pauli repulsion between the electron and the ammonia valence electrons. This model, which is directly derived from the *F*-center model in alkali halides, implies that the majority of the unpaired electron density resides in the cavity, with negligible transfer to the frontier orbitals of the solvent. While this model can fit with the 29 MHz ^{14}N isotropic hyperfine constant, assuming that nitrogen 2s orbitals are involved for which a 1540 MHz hyperfine coupling constant for unit occupancy is expected,[47] it is difficult to reconcile, as recently stressed by Shkrob,[5] with the small and *negative* proton isotropic hyperfine interaction detected in the ^1H HYSCORE spectra and from the NMR Knight shifts. This can only be explained if a spin bond polarization mechanism, similar to that present in conjugated carbon Π radicals operates. This implies that the excess electron dwells in a group orbital encompassing three ammonia molecules. This orbital must have almost no *p* character and a node close to the hydrogen atoms. An alternative to the cavity model, based on an early suggestion by Pitzer,[48] later developed by Symons[33] and Edwards,[32] consists thus in considering a linear combination of suitably modified 3s orbitals on nitrogen, which represent the first Rydberg level of ammonia. As pointed out by Edwards for excess electrons in amines a combination of a cavity-like (1s) orbital and a Rydberg-like orbital constructed from nitrogen 3s orbitals may represent a convenient picture to describe ammonia-solvated electrons.[32] This picture is fully supported by our present data. Interestingly, recent calculations for the NH_4 Rydberg molecule have shown that the unpaired electron is allocated in a N 3s orbital and the calculated hyperfine coupling constant to nitrogen falls between 140 and 211 MHz, depending on the method of calculation, while negligible coupling to the proton is found.[49] Moreover, EPR experimental data on rare-gas isolated Li−NH_3 units[50] have shown absence of anisotropy in the N hyperfine interaction and a_{iso} values of about 36 MHz, whereby the spin density on Li is 60%. Considering these data, one may expect the hyperfine coupling constant for unit occupancy of a 3s N orbital to range between 211 and about 90 MHz. In this way the unpaired electron will be largely accounted for by summation of the unpaired electron density over the three 3s N orbitals without the need to invoke excess electron delocalization in the cavity.

From the HYSCORE spectra hyperfine interaction to the second-shell surface ammonia groups are detected. Even though the signs of the hyperfine tensor components are ambiguous, whatever the choice of the sign a far smaller value (±1.3 MHz) is found with respect to the 9 MHz extracted form NMR Knight shift data, which seems to indicate that the distribution function adopted for the interpretation of the NMR data is unrealistic. This may be due to oscillations of the unpaired electron spin density with distance, as observed for shallow defects in

(43) Coluccia, S.; Lavagnino, S.; Marchese, L. *J. Chem. Soc. Faraday Trans. 1* **1987**, *83*, 477.
(44) Echterhoff, R.; Knozinger, E *Surf. Sci.* **1990**, *1−3*, 237.
(45) Jortner, J. *J. Chem. Phys.* **1959**, *30*, 839.
(46) Ogg, R. A. *J. Am. Chem. Soc.* **1946**, *68*, 155.
(47) Fitzpatrick, J. A. J.; Manby, F. R.; Western, C. M. *J. Chem. Phys.* **2005**, *122*, 084312.
(48) Pitzer, S. K. *J. Chem. Phys.* **1958**, *29*, 453.
(49) Chen, F.; Davidson, E. R. *J. Phys. Chem. A* **2001**, *105*, 10915.
(50) Meier, P. F.; Huge, R. H.; Margrave, J. L. *J. Am. Chem. Soc.* **1978**, *100*, 2108.

semiconductors, which, in the absence of a detailed knowledge of the true unpaired electron wave function, make it very difficult to work out detailed models.

Elaborating a structural model for the second ammonia shell is not easy, however, from the experimental data a realistic possibility is that the second shell is constituted by NH_3 molecules adsorbed via N on first neighbors Mg^{2+} ions and hydrogen bonded to first ammonia shell as schematically illustrated in Chart 1.

This arrangement is in fact compatible with the hyperfine coupling deduced from the HYSCORE spectra. Assuming the interaction to be purely dipolar and taking the a_{iso} value positive, a distance of 0.3 nm to the unpaired electron is deduced. This is compatible with the fact that the majority of the spin density would be in N 3s orbitals and the Mg−O distance of 0.205 nm.

4. Conclusions

We have shown by combined UV−vis−NIR and EPR experiments that excess electrons can be stabilized at the surface of MgO by the cooperative effects of the surface electrostatic potential and two or three nitrogen-containing groups. The resulting surface electron−solvent complex genuinely summarize the essential features of solvated electrons in ammonia. This is demonstrated by the broad absorption centered at about 0.74 eV accompanied by distinct CW-EPR spectra allowing the analysis of the first-shell ammonia nitrogens. Isotopic substitution and ESEEM spectra allowed for the first time the detection of the hyperfine coupling to the ammonia protons. The hyperfine coupling is highly anisotropic with a maximum coupling in the order of 5.5 MHz with a small and negative a_{iso} in agreement with NMR Knight shift data and recent theoretical estimates. Moreover, the hyperfine coupling to the remote (second-shell) nitrogen nuclei is directly observed for the first time. From these magnetic resonance data, it emerges that the excess electron is stabilized in surface "pockets" characterized by a C_{3v} symmetry axis, whereby the unpaired electron is localized on a three-coordinated (corner) Mg^{2+} cation and surrounded by three surface ammonia molecules. Low ammonia pressure used during material preparation leads to the observation of a second species whereby the unpaired electron is stabilized by only two surface ammonia molecules, with corresponding larger spin density on the ammonia nitrogens. On the basis of these new data, our analysis is in agreement with a model whereby the "excess electron" resides predominantly on the nitrogen ammonia molecules, at variance with the "classical" cavity model.

We believe that these new data will be of importance in the general field of electron solvation as they provide new specific information on the nature of these entities and detailed parameters to test theory against.

JA903179B